COMPARISON OF VIRTUAL UNENHANCED AND TRUE UNENHANCED ATTENUATION VALUES BY DUAL-ENERGY CT FOR DETECTING INDISTINCT LIVER METASTASES ON CONTRAST-ENHANCED CT

Motoko Sasajima, Koichi Ishiyama, Takahiro Otani, Makoto Koga, Makoto Sugawara, Tomoki Tozawa, Kento Hatakeyama and Manabu Hashimoto

Department of Radiology, Akita University Graduate School of Medicine

(received 15 May 2020, accepted 28 December 2020)

Abstract

Purpose : We aimed to evaluate the differences between true unenhanced (TUE) and virtual unenhanced (VUE) computed tomography (CT) performed by contrast-enhanced CT with dual-energy CT in the assessment of liver metastases that were difficult to visually identify with contrast-enhanced CT.

Materials and methods : Between April 2018 and September 2019, we identified 266 patients with liver metastases who underwent unenhanced and contrast-enhanced CT with dual-energy CT at our institution, and enrolled 43 liver metastases in 19 patients (7.1%) that were indistinct on contrast-enhanced CT. Mean CT attenuation values for liver metastases and liver parenchyma were measured, and differences between the CT attenuation values for liver metastases and liver parenchyma were analyzed using VUE CT and TUE CT.

Results : The mean CT attenuation values for liver metastases and liver parenchyma in VUE CT versus TUE CT were 51.0 vs. 41.0 HU ($p<0.001$) and 58.2 HU vs. 61.2 HU ($p=0.027$), respectively. The differences in CT attenuation values between liver metastases and liver parenchyma were 10.1 HU on VUE CT vs. 19.3 HU on TUE CT ($p<0.001$).

Conclusion : The contrast between lesions and liver parenchyma on VUE CT was significantly lower than that on TUE CT. VUE CT cannot currently replace TUE CT.

Key words : liver metastases, dual-energy CT, virtual unenhanced CT

Introduction

Computed tomography (CT) is often used to screen for liver metastases. Although contrast-enhanced CT usually allows easier identification of more liver metastases than unenhanced CT, some metastases (particularly hypervascular liver metastases) are identified more easily on unenhanced CT[1,2]. Therefore, both unenhanced and contrast-enhanced CT examinations are performed for screening liver metastases in clinical practice.

Modern dual-energy CT (DECT) techniques allow the creation of virtual unenhanced (VUE) CT images from contrast-enhanced CT by using postprocessing algorithms. Recent studies on VUE CT have shown that the attenuation values of some normal organs under VUE CT are close to those for true unenhanced (TUE) CT[3-10], and many reports have suggested that the error of VUE CT

Corresponding author : Motoko Sasajima MD
Department of Radiology, Akita University Graduate School of Medicine, 1-1-1 Hondo, Akita City, Akita 010-8543, Japan
Tel : +81-18-834-1111
Fax : +81-18-836-2623
E-mail : motoko@med.akita-u.ac.jp

in comparison with TUE CT falls within approximately 10 HU[3-13]. However, only one study examined the usefulness of VUE CT for assessing liver metastases[14]. Thus, the efficacy of VUE CT for detecting liver metastases has not been adequately evaluated. If the diagnosability of VUE CT images with DECT data for liver metastases is not inferior to that of TUE CT, TUE CT could be omitted, thereby reducing the radiation burden on patients and the time required for scanning.

Thus, the purpose of this study was to evaluate the diagnostic ability of VUE CT and TUE CT for liver metastases that are difficult to identify on contrast-enhanced CT by comparing the contrast between liver metastases and normal liver parenchyma on VUE CT and TUE CT.

Materials and methods

Our institutional review board approved this retrospective study (approval number : 2206).

Patients

Between April 2018 and September 2019, we retrospectively identified 266 patients with liver metastases who underwent both unenhanced and contrast-enhanced CT on a DECT system (RevolutionCT ; GE Healthcare, Milwaukee, WI) at our institution. The diagnosis of liver metastasis was clinically determined on the basis of CT data alone without pathological assessments. The CT interpretation report was used to determine whether liver metastases were present. Three diagnostic radiologists retrospectively evaluated the images. In 19 patients (7.1%), liver metastases were judged as difficult to visually identify with portal vein-phase or equilibrium-phase contrast-enhanced CT and easy to find on unenhanced CT. These 19 patients (8 men, 11 women ; mean age, 61.7 years [range, 41-85 years]) with 43 lesions were included and evaluated in the present study. The primary lesion was a neuroendocrine neoplasm in five patients, breast cancer and lung cancer in three patients each, and pancreatic cancer, bile duct cancer, rectal cancer, renal cancer, adrenal cancer, and gastrointestinal stromal tumor in one patient each. Seventeen patients received chemotherapy (platinum and topoisomerase inhibitors, molecular targeted drugs, antimetabolites, etc.) and 2 patients were untreated at the time of the CT scan. The characteristics of the study population are provided in Table 1.

CT technique and protocol

All studies were performed using the RevolutionCT single-source rapid kVp-switching spectral CT scanner (GE Healthcare). TUE CT and portal vein-phase or equilibrium-phase contrast-enhanced CT scans were used in the present study. Non-ionic contrast agents (Omunipaque-300 : Daiichi Sankyo, Tokyo, Japan ; Oiparomin-300 or 370 : Konica Minolta, Tokyo, Japan ; Iomeron-350 ; Eisai, Tokyo, Japan ; Iopromide-370 : Fujifilm, Tokyo, Japan ; or Optiray-320 or 350 ; Guerbet, Paris, France) were administered intravenously. The dose of the contrast medium was 540-750 mgI/kg, depending on the patient's body weight and renal function. TUE series were acquired from the liver dome to the iliac crest during inspiratory breath-holding. The DECT mode incorporated rapidly switching 140-/80-kVp tube voltages, a 128×0.625-mm detector configuration, a pitch of 0.992, and a revolution time of 0.6-1.0 s. A fixed current, between 166 and 480 mA, was selected using automated GSI Assist software (GE Healthcare) with a targeted noise index between 9.7 and 10.5 at a 0.625-mm acquisition. Images were reconstructed using a soft-tissue algorithm with a thickness of 1.25 mm and with application of 70% advanced statistical iterative reconstruction. A post-contrast venous-phase series was acquired from the liver dome to the iliac crest during inspiratory or expiratory breath-hold. The DECT mode was the same as that used in the TUE series, except for the use of a fixed current (between 230 and 440 mA).

Post-processing and image analysis

Reconstructed DECT series data were exported into a DECT post-processing workstation (AW server, version 3.2 ext. 2.0 ; GE Healthcare) incorporating VUE software (Material Suppressed Iodine [MSI] ; GE Healthcare). VUE CT images were reconstructed from the portal vein phase or equilibrium-phase datasets. Axial VUE CT images were reconstructed at a thickness of 1.25 mm.

For each patient, a maximum of three liver metastases were selected based on the following conditions : size as

Table 1. Clinical characteristics and CT protocol

Characteristics (n=19)	Value
Age (years), mean (range)	61.7 (41–85)
Sex, n (%)	
Male	8 (42%)
Female	11 (58%)
Body mass index (kg/m^2), mean ± SD	21.2±3.6
Amount of contrast medium (mgI/kg), mean ± SD	595±51
Phase of contrast-enhanced CT, n (%)	
70 s (portal vein phase)	6 (32%)
95 s (equilibrium phase)	5 (26%)
100 s (equilibrium phase)	1 (5%)
180 s (equilibrium phase)	7 (37%)
Maximum tumor size (mm), median (IQR)	21 (15.5–31)
Primary cancer, n (%)	
Neuroendocrine neoplasm	5 (26%)
Breast cancer	3 (16%)
Lung cancer	3 (16%)
Pancreatic cancer	3 (16%)
Bile duct cancer	1 (5%)
Rectal cancer	1 (5%)
Renal cancer	1 (5%)
Adrenal cancer	1 (5%)
Gastrointestinal stromal tumor	1 (5%)
Chemotherapy, n (%)	
Platinum and topoisomerase inhibitor	4 (21%)
Molecularly targeted drug	4 (21%)
Antimetabolite	3 (16%)
Microtubule inhibitor	2 (11%)
Others	4 (21%)
Untreated	2 (11%)

CT=computed tomography ; SD=standard deviation ; IQR=interquartile range.

large as possible, and presenting with lower contrast between the lesion and liver parenchyma on contrast-enhanced CT than on TUE CT. Finally, CT attenuation values on VUE CT and TUE CT were analyzed for the 43 liver metastatic lesions and the surrounding liver parenchyma.

Mean attenuation values for liver metastases and liver parenchyma were measured using VUE CT and TUE CT. The region of interest (ROI) was set to include liver metastases as large as possible, and mean attenuation CT values were calculated. For each series, mean attenuation CT values for liver parenchyma were obtained by placing circular ROIs (diameter, 10 mm) in three areas (right anterior section, right posterior section, and left lateral section). If the patients had undergone hepatectomy, ROIs were placed in the center and periphery of the residual liver.

To examine visibility, the following indicators were analyzed for differences :

(mean CT attenuation value for liver parenchyma on VUE CT) – (mean CT attenuation value for liver metastasis on VUE CT)

(mean CT attenuation value for liver parenchyma on TUE CT) – (mean CT attenuation value for liver metastasis on TUE CT)

CT attenuation profile curves

In VUE CT and TUE CT, lines (5 pixels wide) were drawn across the center of liver metastases, and the CT values on the line were evaluated. CT attenuation values were obtained using ImageJ software[15,16]. CT attenuation profile curves of VUE and TUE CT were graphed as distance on the horizontal axis and CT values on the vertical axis. The width of the margin of liver metastases on VUE and TUE CT was compared. Figure 1 shows a representative example of CT attenuation profile curves for liver metastasis.

Statistical analysis

All numerical data were analyzed using the Wilcoxon signed-rank test. Values of $p<0.05$ were considered statistically significant. All statistical analyses were performed using SPSS version 24.0 software (IBM Corp, Armonk, NY).

Results

Liver metastases

A total of 43 lesions were included in this study. The median size of liver metastases was 21.0 mm (interquartile range [IQR], 15.5-31.0 mm). The mean CT attenuation values for liver metastases were 51.0 HU (IQR, 44.2-54.1 HU) with VUE CT and 41.0 HU (IQR, 37.5-46.6 HU) with TUE CT. Mean CT attenuation values for liver metastases were significantly higher on VUE CT than on TUE CT ($p<0.001$). The details are shown in Table 2.

Image analysis

The mean CT attenuation values for liver parenchyma were 58.2 HU (IQR, 56.3-63.5 HU) on VUE CT and 61.2 HU (IQR, 59.4-64.0 HU) on TUE CT. Mean CT attenuation values for liver parenchyma were significantly lower on VUE CT than on TUE CT ($p=0.027$). Differences in CT attenuation values between liver metastases and liver parenchyma, which were directly linked to detectability, were 10.1 HU (IQR, 3.2-12.8 HU) with VUE CT and 19.3 HU (IQR, 14.0-25.9 HU) with TUE CT. There was a significant difference between VUE CT and TUE CT ($p<0.001$).

CT attenuation profile curves

In the CT attenuation profile curves, median margins of liver metastases were 5 mm (IQR, 3.25-7 mm) on VUE CT and 2 mm (IQR, 2-3 mm) on TUE CT ($p<0.001$).

Discussion

Our study showed that mean CT attenuation values for liver metastases were significantly higher on VUE CT than on TUE CT, and mean CT attenuation values for liver parenchyma were significantly lower on VUE CT than on TUE CT. CT attenuation profile curves showed that the margins of liver metastases were duller on VUE CT than on TUE CT. These results suggest that for liver metastases that appear obscure on contrast-enhanced CT, the visibility on VUE CT is inferior to that on TUE CT.

These inaccuracies in CT attenuation values on VUE CT may be related to the VUE CT reconstruction method. In our study, the multi-material decomposition method developed by GE was used, and this method is

Table 2. Mean CT attenuation values for liver metastases and liver parenchyma

Median (25th, 75th percentiles) CT values (HU)	VUE CT	TUE CT	*p*-value
Liver metastases	51.0 (44.2 to 54.1)	41.0 (37.5 to 46.6)	<0.001
Liver parenchyma	58.2 (56.3 to 63.5)	61.2 (59.4 to 64.0)	0.027
Difference between liver metastases and liver parenchyma	10.1 (3.2 to 12.8)	19.3 (14.0 to 25.9)	<0.001

VUE CT=virtual unenhanced CT; TUE CT=true unenhanced CT; HU=Hounsfield Unit.

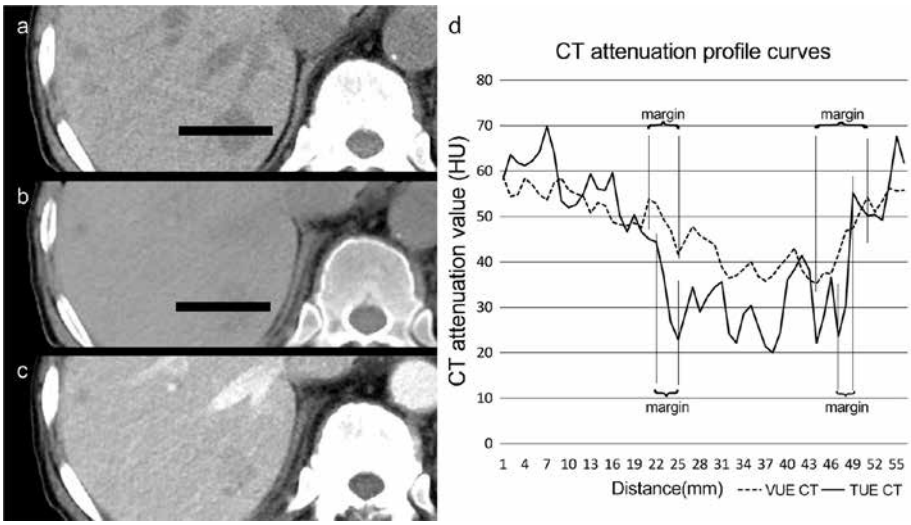

Figure 1. A 68-year-old man with liver metastases from lung cancer. Axial true unenhanced image (a), virtual unenhanced CT image (b), and contrast-enhanced CT image (c). Black lines indicate the CT attenuation profile curves (d). In VUE CT and TUE CT, lines (5 pixels wide) were drawn across the center of the liver metastasis, and the CT values on the line were evaluated. Margins of liver metastases were wider in the VUE CT group than in the TUE CT.

one of the three-material decomposition methods[17]. In the three-material decomposition method, reconstruction is performed by assuming that each voxel is composed of three different materials. In the multi-material decomposition method, three different combinations of the following materials are used depending on the CT value of the voxel : fat, blood, iodine or hydroxyapatite, blood, and iodine. The problem with the three-material decomposition method is that it cannot consider the presence of substances other than fat, hydroxyapatite, blood, and iodine. Previous studies have reported that high concentrations of fat and iodine can cause discrepancies in the CT attenuation values of VUE CT in comparison with TUE CT ; adipose tissue shows higher CT attenuation values with VUE CT than that with TUE CT[3-7,18], and high iodine concentrations show higher[3,8] and lower[4-6] CT attenuation values for VUE CT than for TUE CT. Because of these factors, the use of VUE CT in clinical practice remains limited to date.

Our results show that the CT attenuation values of liver metastases were significantly higher on VUE CT than on TUE CT. This may be due to the substances that constitute liver metastasis or inadequate iodine removal[14]. However, the actual causative factors have not yet been identified. Nevertheless, the material present in liver metastases may be the cause of the higher CT values in VUE CT than in TUE CT. Adipose tissue and high concentrations of iodine, which are known to cause CT attenuation value errors on VUE CT, are unlikely to be present in liver metastases. Liver metastases can cause necrosis and bleeding. Substances in the necrotic tissue or hemorrhage may cause an increase in CT attenuation values on VUE CT compared to TUE CT.

The mean CT attenuation values of liver parenchyma surrounding liver metastases were significantly (approximately 3 HU) lower on VUE CT than on TUE CT. A few reports have shown that the CT attenuation values of the liver parenchyma were significantly lower on VUE CT than on TUE CT[7]. However, in many reports, the CT attenuation values for VUE CT were not significantly different from those for TUE CT[4,8-13] or significantly higher than those for TUE CT[3,5,6,18]. We placed three ROIs at the right anterior section, right posterior section, and left lateral section in the liver and calculated the mean attenuation CT values for liver parenchyma. Most studies calculated the CT values by placing one or two

ROIs in the liver parenchyma[3-5,7-12,18], and a few studies placed three ROIs on the liver parenchyma[6,14]. The present study with three ROIs in the liver parenchyma more accurately represents the CT attenuation value of the whole liver than the study with one or two ROIs in the liver parenchyma. We believe that in comparison with previous studies, our method is more objective for the assessment of CT values of liver parenchyma.

There are some limitations to our study. The main limitation of this study was that it used a single-center, retrospective design and included only a small number of samples. Second, this study used a single-center protocol, and there may have been bias in contrast injection methods. Third, the primary diseases included in the study were biased : neuroendocrine neoplasm, breast cancer, lung cancer, and pancreatic cancer were common. Fourth, the present study did not consider treatment intervention for the patients at the time of the CT scan. Most patients received chemotherapy, which can cause histopathological changes in the liver parenchyma and tumor. These changes may reduce the contrast between liver metastases and liver parenchyma on VUE CT. The image evaluation and clinical application of VUE CT have not been established, and further analyses are needed.

Conclusions

The contrast between liver metastases and liver parenchyma on VUE CT was significantly inferior to that on TUE CT in patients with indistinct liver metastases on contrast-enhanced CT. Therefore, we cannot omit scanning with unenhanced CT when searching for liver metastases with DECT.

Conflicts of interest

The authors have no conflicts of interest to declare.

References

1) Zimmerman, P., Lu, D.S., Yang, L.Y., *et al*. (2000) Hepatic metastases from breast carcinoma : comparison of noncontrast, arterial-dominant, and portal-dominant phase spiral CT. *J. Comput. Assist. Tomogr.*, **24**(2), 197-203.
2) Bressler, E.L., Alpern, M.B., Glazer, G.M., *et al*. (1987) Hypervascular hepatic metastases : CT evaluation. *Radiology*, **162**, 49-51.
3) Toepker, M., Moritz, T., Krauss, B., *et al*. (2012) Virtual non-contrast in second-generation, dual-energy computed tomography : reliability of attenuation values. *Eur. J. Radiol.*, **81**(3), e398-405.
4) Zhang, L.J., Peng, J., Wu, S.Y., *et al*. (2010) Liver virtual non-enhanced CT with dual-source, dual-energy CT : a preliminary study. *Eur. Radiol.*, **20**(9), 2257-2264.
5) Sauter, A.P., Muenzel, D., Dangelmaier, J., *et al*. (2018) Dual-layer spectral computed tomography : Virtual non-contrast in comparison to true non-contrast images. *Eur. J. Radiol.*, **104**, 108-114.
6) Ananthakrishnan, L., Rajiah, P., Ahn, R., *et al*. (2017) Spectral detector CT-derived virtual non-contrast images : comparison of attenuation values with unenhanced CT. *Abdom. Radiol. (NY)*, **42**(3), 702-709.
7) Durieux, P., Gevenois, P.A., Muylem, A.V., *et al*. (2018) Abdominal attenuation values on virtual and true unenhanced images obtained with third-generation dual-source dual-energy CT. *AJR. Am. J. Roentgenol.*, **210**(5), 1042-1058.
8) Borhani, A.A., Kulzer, M., Iranpour, N., *et al*. (2017) Comparison of true unenhanced and virtual unenhanced (VUE) attenuation values in abdominopelvic single-source rapid kilovoltage-switching spectral CT. *Abdom. Radiol. (NY)*, **42**(3), 710-717.
9) Li, Y., Li, Y., Jackson, A., *et al*. (2017) Comparison of virtual unenhanced CT images of the abdomen under different iodine flow rates. *Abdom. Radiol. (NY)*, **42**(1), 312-321.
10) Sommer, C.M., Schwarzwaelder, C.B., Stiller, W., *et al*. (2012) Iodine removal in intravenous dual-energy CT-cholangiography : Is virtual non-enhanced imaging effective to replace true non-enhanced imaging. *Eur. J. Radiol.*, **81**(4), 692-699.
11) Mahmood, U., Horvat, N., Horvat, J.V., *et al*. (2018) Rapid switching kVp dual energy CT : Value of reconstructed dual energy CT images and organ dose assessment in multiphasic liver CT exams. *Eur. J. Radiol.*, **102**, 102-108.

12) De Cecco, C.N., Buffa, V., Fedeli, S., *et al*. (2010) Preliminary experience with abdominal dual-energy CT (DECT) : true versus virtual nonenhanced images of the liver. *Radiol. Med.*, **115**(8), 1258-1266.
13) De Cecco, C.N., Buffa, V., Fedeli, S., *et al*. (2010) Dual energy CT (DECT) of the liver : Conventional versus virtual unenhanced images. *Eur. Radiol.*, **20**(12), 2870-2875.
14) Tian, S.F., Liu, A.L., Liu, J.H., *et al*. (2015) Application of computed tomography virtual noncontrast spectral imaging in evaluation of hepatic metastases : a preliminary study. *Chin. Med. J.*, **128**(5), 610-614.
15) Rasband, W.S. (1997-2012) ImageJ, U. S. National Institutes of Health, Bethesda, Maryland, USA. http://imagej.nih.gov/ij/.
16) Schneider, C.A., Rasband, W.S. and Eliceiri, K.W. (2012) NIH Image to ImageJ : 25 years of image analysis. *Nat. Methods.*, **9**(7), 671-675.
17) Mendonca, P.R., Lamb, P. and Sahani, D.V. (2014) A flexible method for multi-material decomposition of dual-energy CT images. *IEEE Trans. Med. Imaging*, **33**(1), 99-116.
18) Haji-Momenian, S., Parkinson, W., Khati, N., *et al*. (2018) Single-energy non-contrast hepatic steatosis criteria applied to virtual non-contrast images : is it still highly specific and positively predictive. *Clin. Radiol.*, **73**(6), 594.e7-594.e15.